INTERNATIONAL JOURNAL OF ENERGY STUDIES

e-ISSN: 2717-7513 (ONLINE); homepage: https://dergipark.org.tr/en/pub/ijes

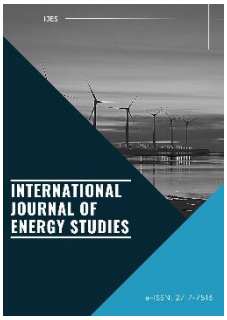

Research Article

Int J Energy Studies 2023; 8(2): 237-250

DOI: 10.58559/ijes.1284416

Received : 17 Apr 2023

Revised : 26 May 2023

Accepted : 26 May 2023

Transverse flux generator design for wind turbine at the rural areas

Engin Hüner*

Energy Systems Engineering, Technology Faculty, Kırklareli Üniversitesi, Kırklareli, Türkiye, ORCID: 0000-0001-5613-5439

*(*Corresponding Author:engin.huner@kırklareli.edu.tr)*

Highlights

- Transverse flux generator was designed for wind turbine
- Analyzes was made via ANSYS Maxwell 3D
- Cogging torque was decreased with optimization core width

You can cite this article as: Hüner E. Transverse flux generator design for wind türbine at the rural areas. Int J Energy Studies 2023; 8(2): 237-250.

ABSTRACT

In this study, transverse flux generator design for micro-wind turbines has been realized. In parallel with the developments in telecommunications in recent years, the use of cell phones and satellite internet has increased. Renewable energy sources are an important candidate to provide energy access and sustainability in rural areas. In this respect, a low-cost, easy-to-build generator that can be produced with 3D printers has been designed. The generator produced has a simple coil and core structure and is a low-cost design. In addition, ANSYS magnetic analyzes were performed together with the 3D solid model of the design. In addition, the core width was optimized and the cogging torque had been improved by 18.29 %.

Keywords: Cogging torque, ANSYS Maxwell, Transverse flux generator

1. INTRODUCTION

The last 20 years have seen rapid changes in the field of telecommunications. The reflections of global communication and the internet on daily life have shaped life and trade in human life. With the Internet, the perspective on trade, communication and professions between countries has developed. Today, many professions can be done by accessing the internet from any location in the world. In this context, access to energy in rural areas has become very important. The most ideal way to provide energy in areas far from the grid is the use of renewable energy sources. Renewable energy sources can be listed as wind energy, solar energy [1], hydroelectric energy, biogas energy [2], thermal energy, wave energy [3-4]. Two of the most important renewable energy sources are wind and solar energy [5] The production of solar energy is based on panels produced by utilizing semiconductor technology [6]. Solar panels are important for energy generation in rural areas due to their semi-flexible and flexible structure and power density. However, weather conditions (e.g. cloudy weather) negatively affect power generation. Therefore, wind turbines are also important for power generation in rural areas [7].

Wind turbines can range from portable structures with a few watts of power to very large-scale mega-watt turbines. As the power of wind turbines increases, production costs and installation costs increase. However, long-term feasibility studies are required for the installation of high-power wind turbines [8-9]. The basis of wind turbine feasibility studies is the collection of long-term wind data for at least one year from the location deemed appropriate. Therefore, both the initial investment cost of energy is high and connecting the generated energy to transmission lines is a costly process.

Wind turbines consist of two basic parts: blades and generators. Generators to be used in wind turbines can be listed as permanent magnet or electric energy-excited due to their excitation structures. In addition, radial or axial flux structures can be applied in terms of flux directions. The generator structure to be designed for small power energy requirement in rural areas can be various. In the literature, small power generators proposed are radial and axial flux permanent magnet DC generators, respectively. In recent years, optimization studies on axial flux permanent magnet (AFPM) generators, methods to reduce the cogging torque, and studies on prototype productions have been intensive. The generators prototyped are multi-rotor and stator PM generators [10], transverse-flux PM generator design with natural cooling and fall back [11], dual rotor V-shaped magnetic pole [12], hybrid excitation claw-pole generator [13], a novel axial-

transverse flux PM synchronous machine [14]. When the techniques to reduce the cogging torque are examined, some studies have mentioned Halbach array [15], using magnet segmentation method [16], influence of the magnetic shape on the cogging torque [17], sinusoidal shaped rotor to reduce torque ripple [18]. However, optimization methods are related to the application of genetic algorithms to open slot AFPM generator [19], a new artificial neural network model with variable air gaps [20], determination of the optimum rotor/stator diameter ratio [21], respectively. In addition, small power permanent magnet generator structures are generally direct drive [22].

In this study, a transverse flux permanent magnet generator is designed for a micro-scale wind turbine using 3D solid modeling. The design is simple and suitable for 3D printer manufacturing. In addition, magnetic analysis of the designed generator was performed with ANSYS Maxwell using the finite element method. The main objectives of the design are low-cost, high-power density and suitable for 3D manufacturing.

2. MATERIAL AND METHOD

The main purpose of the design can be listed as simple structure, cheap cost, and suitability for production with 3D printer. Because the easiest way to access energy in rural areas is to utilize renewable energy sources. In this respect, it is important to obtain electrical energy from wind energy. In this study, a permanent magnet transverse flux generator is proposed for a micro wind turbine with the proposed design. The proposed generator structure is simple with one coil. In transverse flux generators, the flux moves along the magnetic circuit. Therefore, the magnetic flux around the coil moves through the iron core.

2.1. 3D Model of Design

The stator, rotor dimensions and air gap between stator-rotor are calculated by using dimensioning methods based on analytical expressions commonly known in the literature. The rated torque value (T) going to generator consumption, taking into account the parameters rated power (P), efficiency (η) and rated revolutions per second (n) of the targeted generator design;

$$T = (P/\eta) / (2.\pi . n) \quad (1)$$

According to the tangential stress value ($\sigma Ftan$) and T parameters allowed in the design, the volume of the rotor (Vr);

Vr = T / 2. $\sigma Ftan$ (2)

Nominal frequency (f) and number of pole pairs (p), in terms of n;

P= f/n (3)

dimensional ratio χ depending on p;

χ = (π.$\sqrt{p}$) / (4.p) (4)

rotor diameter (Dr) depending on χ and Vr ;

$$Dr = \sqrt[3]{\frac{4.Vr}{\pi.\chi}} \quad (5)$$

The equivalent length of the kernel in χ and Dr (l');

l' = χ.Dr (6)

The length of the air gap between the stator and the rotor, which is a function of p (δ);

δ = (0,18+0,006.P0,4) / 1000 (7)

In Dr and δ, the stator inside diameter (Ds);

$Ds = Dr + 2.\ \delta$ (8)

From the values of l and δ, the net length of the rotor core (l);

$l = l' - 2.\ \delta$ (9)

is calculated. Parameter values were determined according to the formulas in Table 1.

The stator and rotor parameters of the transverse flux generator are given in table 1.

Table 1. Physical dimension of transverse flux generator

Parameter	Value
Stator outer diameter	190 mm
Stator inner diameter	70 mm
Coil section area	64 mm^2
Coil dimension	8x8x14 mm
Iron core number	18
Winding type	Toroidal
Pole number	18
Maximum flux density in the stator core	1.8 Tesla
Magnet dimension	30x10x5 mm
Magnet type	NdFeBr
Inner diameter (Fixed magnet)	70 mm
Outer diameter (Fixed magnet)	130 mm
Inner diameter to outer diameter (λ) for magnet	0,538

The ½ stator of the generator proposed in this study is given in Figure 1. The stator consists of a total of 18 iron cores. The dimensions of each iron core are given in figure 1. The core structure consists of two parts and each iron core is composed of 0.35 mm siliceous sheets. Thanks to its iron core structure, it is suitable for mass production and has a low-cost structure.

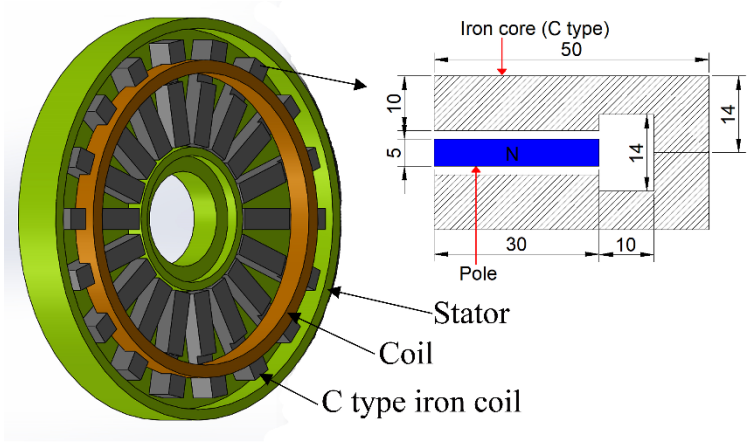

Figure 1. Stator of transverse flux generator

Figure 2 shows the ¼ solid model of the transverse flux generator. The rotor of the generator is designed to be produced from PLA material with a 3D printer and has an 18-pole structure. In the design of the generator, the number of poles and the number of cores is equal to each other. The poles consist of rectangular neodymium magnets. Therefore, the permanent magnet rotor is also designed as low cost.

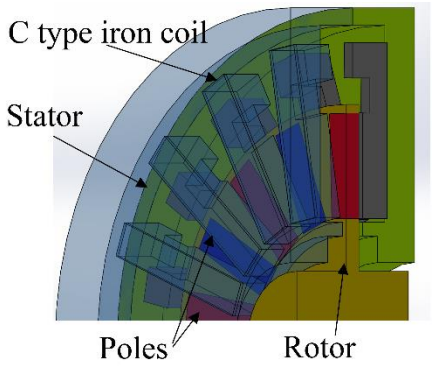

Figure 2. Transverse flux generator ¼ solid model

2.2. Magnetic Equilavent Circuit of the Design

The magnetic equivalent circuit of the transverse flux generator is given in Figure 3. As shown in Figure 3, the magnetic equivalent circuit consists of the magneto motor force generated by the poles, air gap reluctance, iron core reluctance and winding magneto motor force.

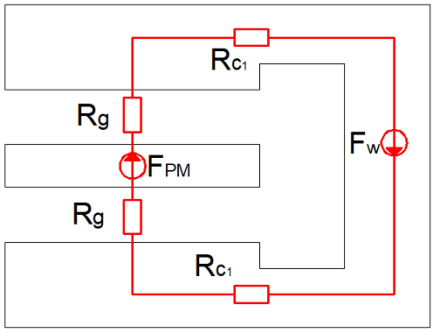

Figure 3. Magnetic equivalent circuit of the transverse flux generator

Considering the equivalent circuit given in Figure 3, the reluctances are given in equations 1, 2, and 3 respectively. In Equations 1, 2, and 3; R_{c_1}, l_1, μ_c, S, R_g, l_g, μ_0, S_0, R_e are given as core reluctance, core length, core permeability, cross section, air gap reluctance, air gap length, air gap permeability, air gap cross section, and equivalent reluctance, respectively.

$$R_{c_1} = \frac{l_1}{\mu_c . S} \quad (1)$$

$$R_g = \frac{l_g}{\mu_0 . S_0} \quad (2)$$

$$R_e = 2.R_{c_1} + 2.R_g \quad (3)$$

Equations 4 and 5 are the magneto-motor forces generated by the magnet and the winding. F_{PM}, B_r, l_{PM}, $\mu_{r_{PM}}$, μ_0, F_w, N, $ve\ i$, are the magnet magneto motor force of the magnet, the magnetic flux value of the magnet, the thickness of the magnet, the relative permeability of the magnet, the permeability of the gap, the magneto motor force of the winding, the number of turns and the current value, respectively.

$$F_{PM} = \frac{B_r . l_{PM}}{\mu_{r_{PM}} \mu_0} \quad (4)$$

$$F_w = N . i \quad (5)$$

2.3. Maxwell Model of the Design

The magnetic analysis of the generator designed to meet the micro-scale energy needs in rural areas was carried out with ANSYS Maxwell. ANSYS Maxwell is a program that uses the finite element method. The 3D model of the generator to be designed in ANSYS Maxwell is given in Figure 4. The transverse flux generator shown in Figure 4 has a single rotor structure between two stators. There is a single toroidal winding in the generator.

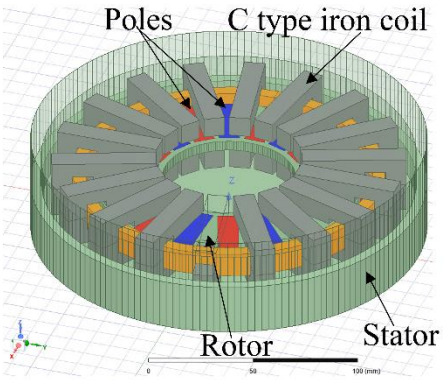

Figure 4. ANSYS Maxwell model

2.4. Magnetic Analyses

Magnetic analysis of the designed TF generator was performed with ANSYS Maxwell 3D. In the design, the rotor is rotated at equal angles and the values of the cogging torque on the rotor are obtained. In addition, the variation of the magnetic flux in the air gap was analyzed.

Figure 5 shows the variation of the cogging torque in the rotor as a result of the interaction of the core and magnets when there is no energy in the winding. The maximum and minimum points of the cogging torque are m1=11.66 Nm and m2=12.33 Nm, respectively.

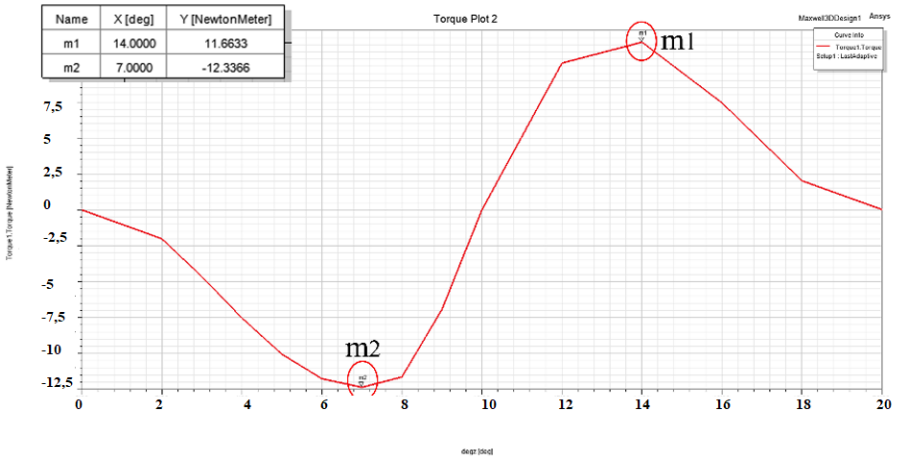

Figure 5. Torque of the proposed TF generator

In Figure 6, the magnetic flux distribution in the rotor iron core of the proposed design is given for the start (0°), near maximum points (6°-8°), zero point (10°), positive maximum point (14°), and end point (20°). When Figure 5 and Figure 6 are examined, it is seen that the maximum cogging torque is at 7°-14° points. The points where the cogging torque is maximum are the points where the magnets are separated from the stator legs and aligned to the other stator leg.

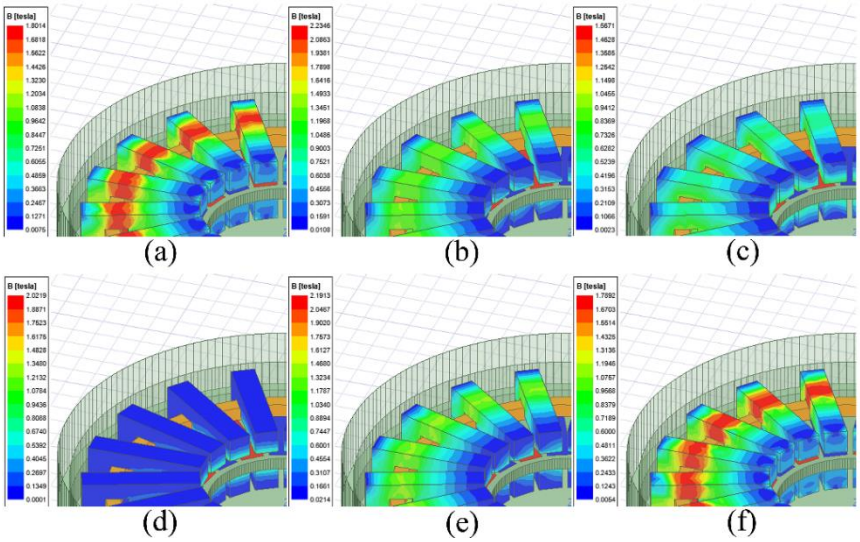

Figure 6. Magnetic flux density on the core a) 0° b) 6° c) 8° d) 10° e) 14° f) 20°

Figure 7 shows the variation of the air gap magnetic flux for the points where the cogging torque is maximum. At the points where the cogging torque is maximum in the negative direction, the maximum values of the air gap are m1=648.1 mT, m2=792.7 mT, respectively.

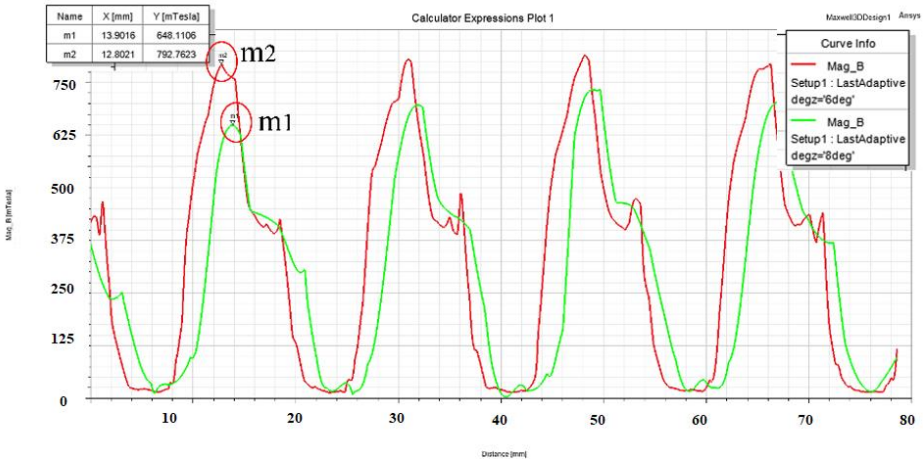

Figure 7. Airgap flux density of the proposed TF generator

2.5. Optimization of Core Width

Optimization of the core width of the designed TF generator was performed with ANSYS Maxwell 3D. Optimization values for core widths of 5, 6, 7, 8, 9, and 10 mm are given in Figure 8.

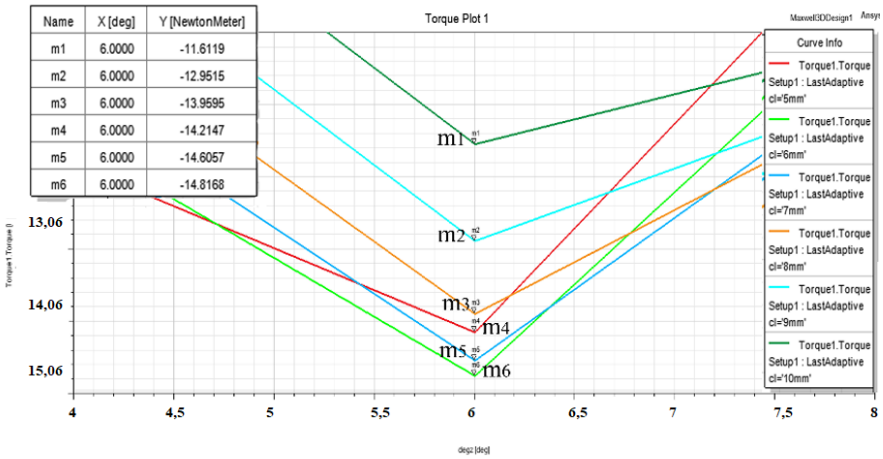

Figure 8. Optimization of core width

In Figure 8, maximum cogging torque values were obtained at 6 degrees. These values are given in Table 2. The obtained values were compared with the percentage changes according to the 5 mm core width. As given in Table 2, the percentage changes relative to 5 mm for 6, 7, 8, 9, and 10 mm core widths are 4.29, 2.82, -1.76, -8.87, and -18.29, respectively. Therefore, the minimum cogging torque was obtained for the 10 mm core width.

Table 2. The effect of core width on cogging torque

Core width	Cogging torque (Nm)	Variation (%)
5 mm (m4)	14.21	Compared value
6 mm (m6)	14.82	4.29
7 mm (m5)	14.61	2.82
8 mm (m3)	13.96	-1.76
9 mm (m2)	12.95	-8.87
10 mm (m1)	11.61	-18.29

3. CONCLUSION

In this study, a transverse flux generator is proposed to generate electricity from wind energy in rural areas. The proposed generator has a simple structure and low cost with its single winding and C-shaped core compared to conventional generators. Core-less stator structures are at the forefront in low-cost generator types. However, generators made without iron core have low air gap flux. This has a negative effect on the energy produced. In the proposed generator, the C-shaped legs used in the stator are low-cost to manufacture and allow the magnetic flux to complete the circuit in a way with lower reluctance.

As a result of the magnetic analysis, the cogging torque and air gap magnetic flux values of the proposed TF generator were obtained. In order to obtain energy in the TF generator, it is sufficient for the air gap flux to be higher than 0.5 Tesla. In addition, since the maximum value of the cogging torque is 14.21 Nm for 5 mm (core leg width). Many methods have been given in the literature to reduce the cogging torque. Analysis was performed by changing the core width parameter value. Optimization has been made for the core width with ANSYS Maxwell. As a result of the optimization, an improvement of 18.29 % was achieved. In addition, one of the prominent features of this study is that it is flexible enough to be produced with a 3D printer.

In future studies, the C-shaped core structure can be optimized with different methods (Genetic, Taguchi experimental design method, etc.). In addition, different combinations of magnet and number of core legs can be compared.

NOMENCLATURE

AFPM	Axial flux permanent magnet
PM	Permanent magnet
PLA	Poliaktik asit
R_{c1}	Core reluctance
l_1	Core length
μ_c	Core permeability
S	Cross section
R_g	Air gap reluctance
l_g	Air gap length
μ_o	Air gap permeability
S_0	Air gap cross section
R_e	Equivalent reluctance
F_{PM}	The magnet magneto motor force
B_r	The magnetic flux value of the magnet
l_{PM}	Thickness of the magnet
μ_{rPM}	The relative permeability of the magnet
F_w	The magneto motor force of the winding
N	The number of turns
TF	Transverse flux

DECLARATION OF ETHICAL STANDARDS

The author of the paper submitted declares that nothing which is necessary for achieving the paper requires ethical committee and/or legal-special permissions.

CONTRIBUTION OF THE AUTHORS

Engin Hüner: Performed the experiments and analyse the results.

CONFLICT OF INTEREST

There is no conflict of interest in this study.

REFERENCES

[1] Şahin ZR, Dinçer F, Yılmaz AS. Design and simulation of grid connected solar power plant fort he electrical energy needs of a family of four people. International Symposium on Advanced Engineering Technologies (ISADET2) Special Issue 2022; 46-56.

[2] Tırınk S. Calculation of biogas production potential of animal wastes: example of Iğdır province. Journal of the Institute of Science and Technology 2022; 12(1): 152-163.

[3] Demirok HD, Kocer HE. Generation of electrical energy from OWC based wave motion. Ejosat Special issue (ICCEES) 2020; 202-206.

[4] Sulukan E. Wave energy potential assessment for Riva and Foça, Turkey. Politeknik Dergisi 2018;2 1(1): 129-135.

[5] Biçen T, Ayhan Arslan A, Vardar A. Regional solar and wind energy characteristics and it's energy potential in northwest of Turkey. Gümüşhane Üniversitesi Fen Bilimleri Dergisi 2022; 12 (2): 527-538.

[6] Şahan M, Kaya R. Fotovoltaik piller kullanılarak güneş ışınım şiddetinin beş farklı doğrultuda ölçülmesi. Süleyman Demirel University Faculty of Arts and Science Journal of Science 2022; 17(1): 155-169.

[7] Karakaya O, Demircan B, Balcı ME. Düşük hızlı ve küçük güçlü rüzgar türbinleri için kalıcı mıknatıslı senkron generatör tasarımı. Balıkesir Üniversitesi Fen Bilimleri Enstitüsü Dergisi 2021; 23(2): 434-454.

[8] Artun O. Determination of the suitable areas for the investment of the wind energy plants (WEP) in Osmaniye using Analytical Hierarchy Process (AHP) and Geographic Information Systems (GIS). Avrupa Bilim ve Teknoloji Dergisi 2020; 20: 196-205.

[9] Çakmakçı BA, Hüner E. Evaluation of wind energy potential: a case study. Energy Sources, Part A: Recovery, Utilization, and Environmental Effects 2022; 44(1): 834-852.
[10] Zhang J, Moreau L, Aubry J, Machmoum M. Sizing optimization methodology of tidal energy conversion chain based on double stator permanent magnet generator. Electric Power Components and Systems 2019; 47(9-10): 940-954.
[11] Patel MA, Vora SC. Analysis of a transverse flux permanent magnet generator with fall-back outer rotor design for wind power generation. International Journal of Ambient Energy 2020; 41(11): 1308-1313.
[12] Kumar RR, Chetri C, Devi P, Saket RK, Blaabjerg F, Sanjeevikumar P, Holm-Nielsen JB. Design and characteristic investigation of novel dual-stator v-shaped magnetic pole six-phase permanent magnet synchronous generator for wind power application. Electric Power Components and Systems 2020; 48(14-15): 1537-1550.
[13] Li W, Huang S. Analysis and design of hybrid excitation claw-pole generator. Electric Power Components and Systems 2011; 39(7): 680-695.
[14] Bendib MH, Hachemi M, Marignetti F. Electromagnetic design and analysis of a novel axial-transverse flux permanent magnet synchronous machine. Electric Power Components and Systems 2017; 45(8): 912-924.
[15] Balakrishnan J, Govindaraju C. Multi-phase permanent magnet generator with halbach array for direct driven wind turbine: A hybrid technique. Energy Sources, Part A: Recovery, Utilization, and Environmental Effects 2022; 44(3): 5699-5717.
[16] Ghasemi A. Cogging torque reduction and optimization in surface-mounted permanent magnet motor using magnet segmentation method. Electric Power Components and Systems 2014; 42(12): 1239-1248.
[17] Qiu H, Hu K, Yu W, Yang C. Influence of the magnetic pole shape on the cogging torque of permanent magnet synchronous motor. Australian Journal of Electrical and Electronics Engineering 2017; 14(3-4): 64-70.
[18] Nazir M, Ikram J, Yousuf M, Bukhari SSH, Shah MA, Memon AA, Ro JS. Investigation of sinusoidal shaped rotor to reduce torque ripple in axial flux permanent magnet machine. International Journal of Ambient Energy 2022; 43(1): 8113-8122.
[19] Hüner E, Toylan H. Design optimization with genetic algorithm of open slotted axial flux permanent magnet generator for wind turbines. International Journal of Green Energy 2023; 20(4): 423-431.

[20] Tekerek A, Kurt E, Tekerek M. A new artificial neural network model for the output voltage and power predictions of permanent magnet generators with variable air gaps. Electric Power Components and Systems 2022; 50(19-20): 1131-1142.
[21] Chaaban FB. Determination of the optimum rotor/stator diameter ratio of permanent magnet machines. Electric Machines & Power Systems 1994; 22(4): 521-531.
[22] Zhang Z, Nilssen R, Muyeen SM, Nysveen A, Al-Durra A. Design optimization of ironless multi-stage axial-flux permanent magnet generators for offshore wind turbines. Engineering Optimization 2017; 49(5): 815-827.
[23] Pyrhonen J, Jokinen T, Hrabovcova V. Design of rotating electrical machines. John Wiley & Sons 2013.